



Plasma and platelet lipidome changes in Fabry disease

Bo Burla^{a,1,*}, Jeongah Oh^{b,c}, Albina Nowak^{d,e}, Nathalie Piraud^f, Eduardo Meyer^g, Ding Mei^b, Anne K. Bendt^a, Jan-Dirk Studt^h, Beat M. Frey^g, Federico Torta^{a,b}, Markus R. Wenk^{a,b,i,*}, Pierre-Alexandre Krayenbuehl^{e,j,*}

^a Singapore Lipidomics Incubator, Life Sciences Institute, National University of Singapore, Singapore

^b Precision Medicine Translational Research Program and Department of Biochemistry, Yong Loo Lin School of Medicine, National University of Singapore, Singapore

^c NUS Graduate School for Integrative Sciences and Engineering, National University of Singapore, Singapore

^d Department of Internal Medicine, Psychiatric University Clinic Zurich, Switzerland

^e Department of Endocrinology, Diabetology and Clinical Nutrition, University Hospital Zurich, Switzerland

^f HTHC High Tech Home Care AG, Rotkreuz, Switzerland

^g Swiss Red Cross (SRC), Zurich-Schlieren, Switzerland

^h Division of Medical Oncology and Hematology, University Hospital Zurich, Zurich, Switzerland

ⁱ College of Health and Life Sciences, Hamad Bin Khalifa University, Doha, Qatar

^j General Practice Brauereistrasse, Uster-Zurich, Switzerland

ARTICLE INFO

Keywords:

Fabry disease
Gb3
Lipidomics
Lysosomal storage disease
Platelets
Sphingadiene

ABSTRACT

Background: Fabry disease (FD) is an X-linked lysosomal storage disorder characterized by the progressive accumulation of globotriaosylceramide (Gb3) leading to systemic manifestations such as chronic kidney disease, cardiomyopathy, and stroke. There is still a need for novel markers for improved FD screening and prognosis. Moreover, the pathological mechanisms in FD, which also include systemic inflammation and fibrosis, are not yet fully understood.

Methods: Plasma and platelets were obtained from 11 ERT (enzyme-replacement therapy)-treated symptomatic, 4 asymptomatic FD patients, and 13 healthy participants. A comprehensive targeted lipidomics analysis was conducted quantitating more than 550 lipid species.

Results: Sphingadiene (18:2;O2)-containing sphingolipid species, including Gb3 and galabiosylceramide (Ga2), were significantly increased in FD patients. Plasma levels of lyso-dihexosylceramides, sphingoid base 1-phosphates (S1P), and GM3 ganglioside were also altered in FD patients, as well as specific plasma ceramide ratios used in cardiovascular disease risk prediction. Gb3 did not increase in patients' platelets but displayed a high inter-individual variability in patients and healthy participants. Platelets accumulated, however, lyso-Gb3, acylcarnitines, C16:0-sphingolipids, and S1P.

Conclusions: This study identified lipidome changes in plasma and platelets from FD patients, a possible involvement of platelets in FD, and potential new markers for screening and monitoring of this disease.

1. Introduction

Fabry disease (FD; OMIM #301500) is an X-linked lysosomal storage disease characterized by mutations of the *GLA* gene encoding for the enzyme α -galactosidase A (α -Gal A) that hydrolyses the terminal α -1,4-galactosyl moiety from glycosphingolipids such as

globotriaosylceramide (Gb3) and galabiosylceramide (Ga2) (Fig. 1). Reduced activity or altered specificity of α -Gal A leads to a systemic accumulation of Gb3 causing tissue damage [1]. In classic FD, males have no or only marginal α -Gal A activity and onset of symptoms often starts during childhood and progresses to kidney diseases, cardiomyopathies, and cerebrovascular symptoms [1,2]. Heterozygous females

* Corresponding authors at: Singapore Lipidomics Incubator (SLING), Life Sciences Institute, National University of Singapore, 28 Medical Drive, 117456, Singapore (B. Burla); College of Health and Life Sciences, Hamad Bin Khalifa University, Doha, Qatar (M. R. Wenk); Department of Endocrinology, Diabetology and Clinical Nutrition, University Hospital Zurich, Rämistrasse 100, 8091 Zurich, Switzerland (P.-A. Krayenbuehl).

E-mail addresses: bo.burla@nus.edu.sg (B. Burla), bchoj@nus.edu.sg (J. Oh), albina.nowak@usz.ch (A. Nowak), mwenk@hbku.edu.qa (M.R. Wenk), pierrea.krayenbuehl@usz.ch (P. Krayenbuehl).

¹ Joint corresponding authors.

<https://doi.org/10.1016/j.cca.2024.119833>

Received 16 January 2024; Received in revised form 14 June 2024; Accepted 24 June 2024

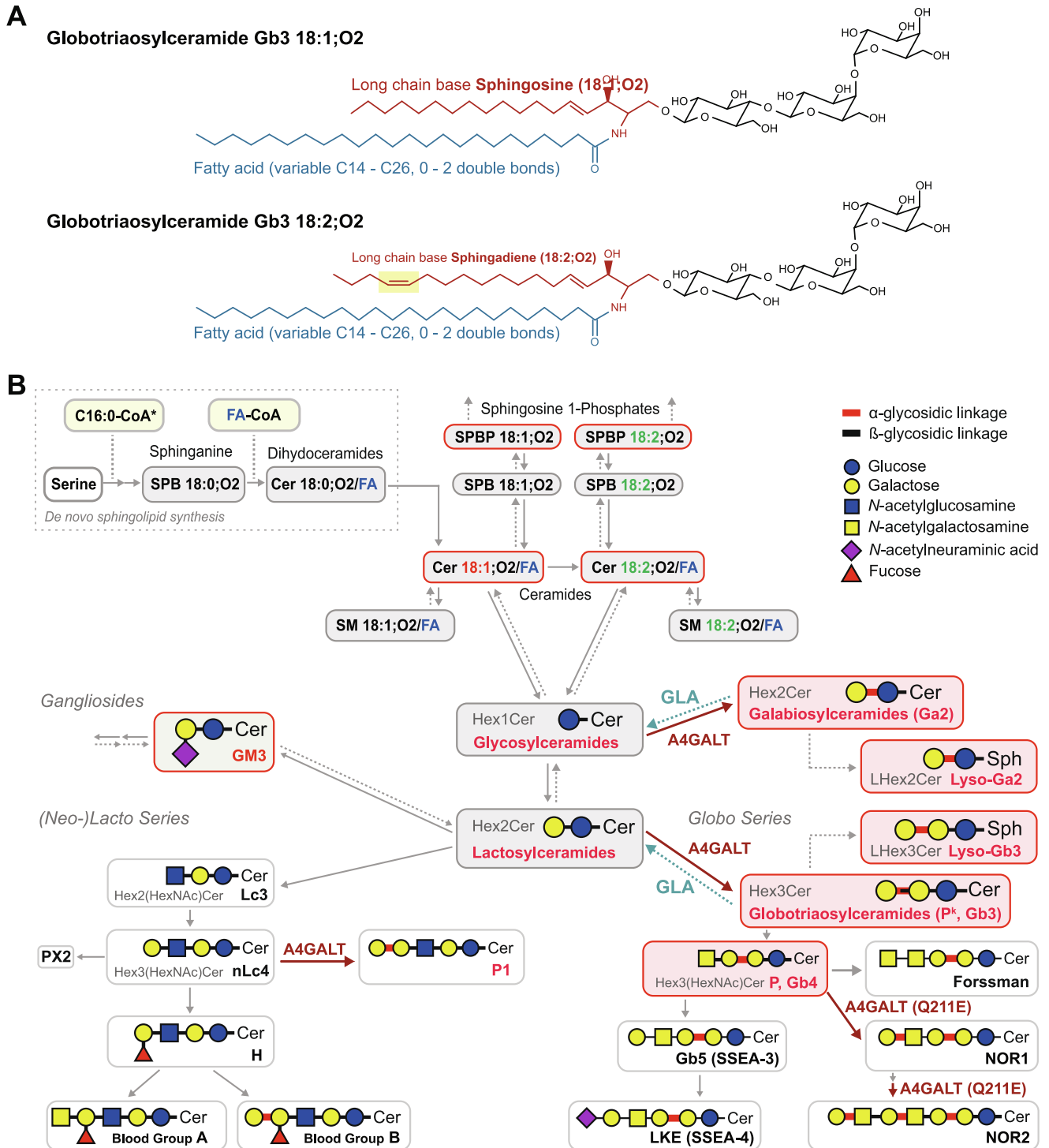
Available online 30 June 2024

0009-8981/© 2024 The Authors. Published by Elsevier B.V. This is an open access article under the CC BY license (<http://creativecommons.org/licenses/by/4.0/>).

with classic FD have more variable disease expression that can be mild or as severe as in males. In so-called later-onset FD, residual α -Gal A activity is still present. Symptoms occur later in life and are often milder or limited to specific organs, i.e., heart or kidneys [3]. Specific severe symptoms, such as stroke, may also be initial, or even sole, symptoms of FD [4–7]. Prevalence estimates across sexes range from 1:40,000 to 1:200,000 for classic, and 1:1,250 to 1:5,500 for later-onset FD variants

[8]. Treatment of FD includes enzyme replacement therapy (ERT) and pharmacological chaperones [3,9].

Diagnosis of FD typically involves measurement of α -Gal A activity in dried blood spots, plasma, and leukocytes, and sequencing of the *GLA* gene [10,11]. Analysis of Gb3, or its deacylated form, lyso-Gb3, can support the diagnosis when a *GLA* variant of unknown pathogenicity was identified [3,12,13]. Lyso-Gb3 is considered superior to total Gb3 in



the diagnosis and prognosis of FD, especially in heterozygous females [14–17]. While typically total levels are measured [18–20], specific Gb3 and lyso-Gb3 molecular species appear to have partially different roles in FD pathogenesis and thus may also have distinct utilities in diagnosis and monitoring of FD [21,22].

The pathological processes in FD extend beyond local tissue damage from Gb3 accumulation and include systemic changes, such as inflammation, increased levels of proinflammatory cytokines, signatures of extracellular matrix remodeling, endothelial dysfunction, and fibrosis. An increased platelet activity and a prothrombotic state was also reported [23–25]. Many of these pathological processes have been shown to alter plasma lipid profiles in other diseases [26,27], suggesting lipiome alterations also in FD.

In this study we aimed to (i) comprehensively profile different Gb3 molecular species in human plasma and platelets as potential FD marker, and (ii) analyze whether the systemic changes in FD are reflected in the plasma and platelet lipidome beyond Gb3 and its metabolites.

2. Materials and methods

2.1. Subjects

This study has been approved by the ethics committee of the canton of St. Gallen, Switzerland (EKSG 15/008) and by the Institutional Review Board of the National University of Singapore (NUS-IRB B-16-025). The study has also been registered at [ClinicalTrials.gov](https://clinicaltrials.gov) (NCT02649660) and was conducted in accordance with the principles of the Helsinki Declaration. All participants gave written informed consent to donate samples for this research study.

Plasma, serum, and platelet samples were obtained from a total of 15 FD patients and 13 healthy study participants (Table 1, Table S1). All FD patients had a confirmed *GLA* mutation. Asymptomatic female FD patients in this study had no FD-related symptoms. All symptomatic FD patients received ERT according to local guidelines, given intravenously every 2 weeks at the licensed dose of either recombinant agalsidase- α (Replagal, 0.2 mg/kg) or agalsidase- β (Fabrazyme, 1 mg/kg). None of the patients were treated with pharmacological chaperones. Healthy participants were recruited from volunteers and have self-declared to be without known cardiovascular, cerebrovascular, and renal diseases, and conditions of platelet function, blood coagulation and lipid metabolism.

2.2. Sample collection

Blood samples were collected from non-fasted control participants,

and from non-fasted FD patients immediately before the ERT infusion during home therapy or in the clinic. To minimize pre-analytical biases [28], individual samples, or batches of 2 to 4 samples from control subjects and FD patients were co-collected in a stratified manner, and subsequently co-processed. Blood used for platelet and plasma isolation was collected into 4.5 mL BD Vacutainer tubes containing citrate solution (0.109 mol/L). For serum, blood was drawn into BD Vacutainer Serum tubes spray-coated with silica. Collected blood samples were kept at room temperature (RT) for 2 to 4 h before further processing and clinical laboratory analyses. Platelet-poor plasma and serum was collected after centrifugation at 2000 g for 10 min (4 °C) and stored at –80 °C.

2.3. Clinical laboratory analyses and clinical data collection

From all participants a full blood count, as well as serum alanine transaminase (ALAT), C-reactive protein (CRP), serum albumin, serum creatinine, serum total cholesterol, HDL-C, LDL-C and TAG were determined in the clinical laboratory from collected blood samples (Table S1). eGFR (estimated glomerular filtration rate) was calculated from serum creatinine using the 2021 CKD-EPI equation [29]. Clinical data of the FD patients were obtained from medical records (Table S2).

2.4. Platelet isolation

Platelet isolation from whole blood was based on a modified differential centrifugation method in presence of the CTAD anti-coagulant mixture [30,31]. First, 625 μ L TAD 10x solution (15 mmol/L theophylline, 3.7 mmol/L adenosine, 198 μ mol/L dipyridamole, in Dulbecco's phosphate-buffered saline [DPBS]) was pipetted directly into the Vacutainer containing citrated whole blood and mixed by inverting 6 times. Platelet-rich plasma (PRP) was then obtained by centrifugation at 120 g for 10 min, without brake (Sorvall Legend RT+) at RT (~22 °C). The PRP was transferred to a 5 mL polypropylene (PP) tube and mixed with 0.01 vol apyrase 2 U/mL and 1 vol TAD 2x/DPBS. After centrifugation (80 g, 10 min, without brake, RT), the supernatant was transferred to a 2 mL PP tube, and centrifuged again (1000 g, 10 min, brake 2, RT). The supernatant was discarded and the platelet pellet was washed twice by resuspending in 2 mL TAD 2x/PWD (TAD 10x diluted 1:5 v/v in Platelet Wash Buffer (140 mmol/L NaCl, 10 mmol/L NaHCO₃, 2.5 mmol/L KCl, 0.5 mmol Na₂HPO₄, 1 mmol/L MgCl₂, 6.46 mmol/L trisodium citrate, 1 g/L D(+)-glucose, pH 6.5, adjusted with NaH₂PO₄), centrifugation (750 g, 10 min, RT, brake 2) and discarding supernatants. The pellet was finally resuspended in 1 mL TAD 2x/PWD and platelet

Table 1

Biographic and clinical characteristics of the Fabry patients. FD Type: Fabry disease type, asympt: asymptomatic for FD, Mutations: missense, unless tagged with X indicating frameshift or nonsense mutations, ERT: Under enzyme replacement therapy, eGFR: estimated glomerular filtration rate (mL/min/1.73 m²; reference range \leq 90), LVMMI: left ventricular myocardial mass index (g/m²; \leq 115 for males, \leq 95 for females). Point Label indicates the label used in the plots to highlight specific subjects. * denotes values outside the reference range. Stroke: stroke or transient ischemic attack. # Denotes the patient who had a kidney transplant before participating in this study.

ID	Sex	Age	FD type	Mutation	ERT	eGFR	LVMMI	Stroke	Neuropathy	Point Label
01A	M	30	Classic	Ins353T ^X	+	*40	86			X
03C	M	34	Classic	M42T	+	*71	87		+	X
11 K	M	36	Classic	M42T	+	#(92)	103		+	T
07G	M	29	Classic	R227X ^X	+	126	66			X
13 M	M	64	Later-onset	N215S	+	*79	NA			
26Z	M	46	Later-onset	R301Q	+	*85	105	+	+	
09I	F	57	Classic	D266Y	+	97	59	+		+
10 J	F	29	Classic	S345P	+	111	59			
12L	F	56	Classic	D266Y	+	*71	*104			*
21U	F	42	Classic	640-3C > G	+	112	50	+	+	
22 V	F	69	Classic	T194I	+	*73	*174	+		a
02B	F	32	Classic/asympt.	Ins353T ^X		107	52			X
04D	F	38	Classic/asympt.	T194I		100	53			
05E	F	40	Classic/asympt.	T194I		104	66			
18R	F	42	Benign/asympt.	N139S		112	44			

count was determined using a Sysmex hematology analyzer. Aliquots, containing 150 million platelets each, were transferred to 2 mL PP tubes and centrifuged (750 g, 10 min, no brake, RT) in a microcentrifuge. After discarding the supernatant, pellets were frozen and stored at -80°C .

2.5. Lipid extraction and derivatization

Platelet isolates (pellets of 150 million cells) were extracted in 300 μL 1-butanol:methanol 1:1 (v/v) containing internal standards (ISTD; Table S3) by vortexing (30 s), followed by sonication in an ultrasonic bath for 30 min at $10\text{--}20^{\circ}\text{C}$ [32]. For plasma and serum, 20 μL was mixed with 200 μL 1-butanol:methanol 1:1 (v/v) containing ISTDs (Table S3), and extracted as platelets. After centrifugation (14,000 g, 15 min, 4°C), aliquots of the supernatants were transferred to PP autosampler vials for subsequent analyses. Another aliquot (50 μL) of each sample was diluted with 50 μL methanol and derivatized with 30 μL (trimethylsilyl)diazomethane (TMS) (2 M in hexanes, Sigma-Aldrich) for 20 min at 25°C and 700 rpm (Thermomixer, Eppendorf, Germany). The reaction was stopped by adding 1 μL acetic acid 100%. After centrifugation (14,000 g, 10 min, 4°C), supernatants were transferred to autosampler vials for subsequent S1P analysis. All extractions were performed twice using different sample aliquots, the first extraction series (platelets, plasma, serum) was used for Gb3, Gb4 and S1P analyses, the second (platelets and plasma only) for the sphingolipid panel and the general lipid panel (phospholipids, neutral lipids, acylcarnitines). For one subject (F07G), insufficient platelet isolate was available for the second extraction series and thus only Gb3, Gb4 and S1P were analyzed in platelets. For serum lyso-Gb3/lyso-Hex2Cer (LHex2Cer) analyses, 20 μL serum was extracted as described above with 200 μL 1-butanol:methanol 1:1 (v/v) containing 25 $\mu\text{mol/L}$ *N*-glycinated lyso-Gb3 (Matreya LLC, #1530). A 50 μL aliquot of each extract was transferred to an PP autosampler vial, dried down using a SpeedVac concentrator and reconstituted in 35 μL 2-propanol:hexane:water 10:5:2 (v/v/v) with 5 mL/L formic acid (IWHF) [33]. For serum Ga2 analysis, 50 μL aliquots of stored serum extracts prepared for Gb3 analysis (see above) were dried and reconstituted in 35 μL IWHF. For platelet lyso-Gb3/LHex2Cer and Ga2 analyses, 40 μL aliquots of stored platelet extracts prepared for Gb3 analysis (see above) were dried and reconstituted in 30 μL IWHF. As retention time reference for the Ga2 analysis, 100 μL of an urine extract from a male healthy volunteer, prepared as described by Boutin et al. [34], was dried and reconstituted in 30 μL IWHF. All reconstituted extracts were used for LC-MS analyses.

BQC (Batch Quality Control) samples, generated by pooling equal volumes of each plasma or serum sample, were co-extracted and measured together with study samples at regular intervals. Process blank samples (PBLK), not containing any matrix, were also co-processed with the samples. TQC (Technical instrument Quality Control) samples were prepared by pooling aliquots of the extracts or derivatives, respectively. Response QC (RQC) samples were obtained by serial dilution of TQCs with 1-butanol:methanol (1:1, v/v), or by using different TQC injection volumes.

2.6. LC-MS analyses

All lipid species were measured using targeted multiple reaction monitoring (MRM)-based LC-MS methods on different platforms using Agilent 6495 series triple quadrupole (QQQ) mass spectrometers. Detailed information on the used LC-MS protocols are available from Table S4-S10. The method by Muralidharan et al. [35] was adapted for analysis of Gb3 and Gb4, while other sphingolipids were analyzed using a method by Burla et al. [36], both with modified transition lists. Analysis of S1P from TMS-derivatized extracts followed the method by Narayanaswamy et al. [36,37], while phospholipids, neutral lipids, and acylcarnitines were analyzed using the method by Huynh et al [38]. Lyso-Gb3 and LHex2Cer were measured using the reversed-phased (RP)-based method reported in Beasley et al [33]. A modified hydrophilic

interaction chromatography (HILIC)-based method published by Boutin et al. [34] was used to analyze isobaric LacCer and Ga2 species.

2.7. Lipidomics data processing

Peak annotation and integration was performed using Agilent MassHunter Quantitative software (Version 10), based on retention time [36,38,39], and in case of sphingolipids (including Gb3) also on qualifiers [36]. Isotopic correction was applied for species that were co-integrated with interfering M+1 or M+2 isotopes [36,40]. Loess-based signal drift correction based on BQCs for plasma and TQCs for platelets (span of 0.75) was applied when it reduced the sample coefficient of variability (CV) [41].

The lipidomics dataset was filtered based on following criteria: (i) signal-to-blank ratio > 3 , based on the sample with lowest intensity, (ii) analytical CV $< 25\%$, except for serum Ga2 with $< 35\%$ (based on TQCs for platelets, and BQCs for plasma), and (iii) linear response of the RQCs with $R^2 > 0.8$. Normalization and quantification were based on corresponding class-specific ISTDs. Final concentrations are given as $\mu\text{mol/L}$ plasma and serum, or amol/platelet, respectively (Tables S11 to S13), but should not be considered as absolute concentrations due to the lack of external calibration and authentic ISTD for most species [42]. The used lipid nomenclature followed the shorthand notation by Liebisch et al., 2020 [43], except for sphingoid base 1-phosphates (SPBP) that were named S1P in the main text. Additional details on the lipidomics analyses are available from the Lipidomics Minimal Reporting checklist [44] (see Supplementary Information and Data Availability).

2.8. Statistical analysis and visualizations

Statistical tests comparing groups were based on two-tailed Student's *t*-test of log-transformed data, if not otherwise stated. Significant differences stated in figures and text are based on $P \leq 0.05$. For comparisons of lipid classes between classic FD and controls, false-discovery rates (FDR) was calculated using Benjamini–Hochberg adjustment [45]. For individual lipid species, the corresponding FDR was based on *q*-values [46], calculated separately for the sphingolipid and general lipid panels. The FDR is indicated in the main figures. Chromatograms (Fig. S6–S9) were plotted using Agilent MassHunter Qualitative (Version 12) and annotated in Microsoft PowerPoint (Version 16) and Adobe Illustrator (Version 28.5). Minor adjustments to annotations in figures were made using Adobe Illustrator. Original figure versions are available from the GitHub repository.

2.8.1. Software

All data processing and analysis was performed using a software pipeline written in R (see GitHub Repository under Data Availability). R version 4.4.0 was used for the actual analysis with following R packages: tidyverse (version 2.0.0), qvalue (2.35), ggsignif (0.6.4), ggplot2 (3.5.1), ggpubr (0.6.0), gt (0.10.1), and patchwork (1.2.0) [47–52].

3. Results

3.1. Clinical characteristics

Plasma and platelet samples were collected from 15 Fabry Disease (FD) patients and 13 control participants (Table 1 and Table S1). All male FD patients were symptomatic and under enzyme replacement therapy (ERT). Two patients had later-onset FD with the cardiac N215S and the renal/cardiac R301Q variants, respectively [53,54]. The female FD groups consisted of 5 symptomatic classic heterozygous patients under ERT treatment, and 4 asymptomatic, untreated patients (Table 1). Female classic symptomatic FD patients were with 50.6 (range 29–69) years considerably younger than control and asymptomatic FD patients, who were 28.4 years (18–42) and 38 (32–43) years old, respectively (Fig. S1 and Table S1). The two youngest, 19 years old, female control

participants and the three oldest female FD patients are labelled with specific symbols in the figures, see Table 1. The male classic FD patients had a similar mean age with 42 (range 30–64) years as the corresponding control participants with 40.5 (30–45) years. Six FD patients had impaired kidney function, based on eGFR, and one had a kidney transplant (Table 1). Cardiac involvement with left ventricular hypertrophy (LVH) [55], based on LVMMI (left ventricular myocardial mass index) was present in two patients (Table 1). N-terminal pro-brain natriuretic peptide (NT-proBNP) was elevated (>125 pg/mL) in 6 of 14 FD patients (Table S2). Strokes or active neuropathy occurred in four patients each (Table 1). The oldest female FD patient had 3 affected organs (Table 1, labelled in plots with an ^a). Participants of the control group had normal clinical laboratory parameters with no significant dyslipidemia, except of one male who had an elevated platelet count (Fig. S1). Male FD patients had lower hematocrit and hemoglobin values (Fig. S1). Furthermore, male patients had lower platelet counts, and increased platelet indices, i.e., PWD (platelet distribution width), MVP (mean platelet volume) and P-LCR (platelet-large cell ratio) (Fig. S1). In the subsequent text, FD patients always refer to as classic FD patients who were under ERT treatment.

3.2. Globotriaosylceramides (Gb3)

In plasma, 15 different Gb3 species were quantified, harboring different long chain bases (LCB) and fatty acids (FA), with one species (Gb3 18:1;O2/17:0) likely representing a methylated Gb3 analog. The total plasma concentration of Gb3 species harboring either of the LCBs sphingosine (18:1;O2) or sphingadiene (18:2;O2) were significantly increased in classic FD patients compared to the controls and asymptomatic FD patients (Fig. 2A). Significant differences were also present when males and females were analyzed separately (Fig. S2A). The differences between the groups were comparable for both Gb3 subclasses, with fold-differences of 2.1 and 1.9 for Gb3 18:1;O2 and Gb3 18:2;O2 for males, and 1.4 and 1.5 for females, respectively (Fig. S2A). On a molecular species level, all 9 Gb3 18:1;O2 and 5 Gb3 18:2;O2 species were significantly increased (Fig. 2B and Fig. S2B). When male and females were analyzed individually, 3 of 9 Gb3 18:1;O2, and 4 of 5 Gb3 18:2;O2 species were significantly increased in both, male and female, classic FD patients, compared to their corresponding controls (Fig. S2C). The 2 male FD patients with frameshift or nonsense *GLA* mutations had the highest Gb3 levels among all subjects (Fig. 2A). The sole FD patient with a kidney transplant had the lowest levels in total, as well as in all, except one, individual Gb3 species, among the male classic FD patients (Fig. 2AB).

In platelets, the total concentrations of Gb3 18:1;O2 and Gb3 18:2;O2 did not differ between the groups (Fig. 3A and Fig. S3A). Among the 10 Gb3 18:1;O2 and 3 Gb3 18:2;O2 molecular species, only Gb3 18:1;O2/16:0 (FDR 40 %) and especially Gb3 18:2;O2/16:0 (FDR 7 %) were significantly higher in classic FD patients (Fig. 3B and Fig. S3BC). In the two later-onset FD patients, the Gb3 18:2;O2/16:0 levels were comparable to the classic ERT group (Fig. 3B). The total Gb3 concentrations did not display any correlation between platelets and plasma, whereas the molecular species Gb3 18:2;O2/16:0 showed a significant correlation (Fig. 3C).

3.3. Inter-individual variability of Gb3

We noticed that the platelet concentrations of Gb3 species span a wide range between samples, also among control participants (Fig. 3B and Fig. S3B). We therefore examined the inter-individual variability of Gb3 in platelets and plasma. In platelets, the coefficient of variation (CV) of long-chain Gb3s, e.g. Gb3 18:1;O2/16:0 and Gb3 18:2;O2/16:0, was 13–50 %, whereas all very long-chain (C20–C26) Gb3 species had CVs between 85 % to 103 % (Fig. 3D). The fold-difference between the highest and lowest concentration (range ratio, RR) of a species ranged from 1.6 to 15.6-fold for long chain, and from 81 to 407 for very long-

chain Gb3 species, (Fig. S4). CVs of these very long-chain Gb3s were lower in FD patients compared to controls (Fig. 3D). In plasma, CVs of Gb3 species were more uniform and lower compared to platelets, with CVs between 27 % and 40 %, and RRs between 2.5 and 4.5 (Fig. 3D and Fig. S4).

3.4. Lyso-Gb3 (globotriaosylsphingosines)

Serum lyso-Gb3 18:1;O2 and lyso-Gb3 18:2;O2 were elevated in all FD groups (Fig. 2C). Fold changes in the classic ERT-treated patients compared to controls, were 53 and 106, respectively, in males, and 21 and 26, respectively, in females. The lyso-Gb3 analogs, lyso-Gb3(-28), lyso-Gb3(18), and lyso-Gb3(34) were also increased (Fig. S5). As observed with Gb3, lyso-Gb3 levels were highest in the two male patients with frameshift or nonsense *GLA* mutations (Fig. 2C). Among the asymptomatic untreated female FD patients, the patients with a missense (Ins353T) and benign (p.N139S) *GLA* mutations (Table 1) had highest and lowest lyso-Gb3 levels, respectively. In platelets, lyso-Gb3 18:1;O2 was also detected, with significantly increased levels in the classic ERT-treated FD patients (Fig. 3E). Based on our literature search, lyso-Gb3 has not been reported in platelets before. The measured levels, however, were low and near the limit of detection (Fig. S6) and none of the lyso-Gb3 analogs were detectable in platelets.

3.5. Galabiosylceramide and Lyso-Hex2Cer

A HILIC-based method was used to separate the isomeric dihexosylceramides (Hex2Cer) species galabiosylceramide (Ga2) and lactosylceramide (LacCer). LacCer constituted the bulk serum Hex2Cer. However, among the four analyzed serum Hex2Cer 18:2;O2 species, low amounts of Ga2 species were also detectable (Fig. S7). The chromatographic peaks had low intensities, near the detection limit, and were prone to interferences from the tailing of the high intensity LacCer peaks eluting before (Fig. S7). Nevertheless, 2 Ga2 species were quantifiable with a CV < 30 %, whereby Ga2 18:2;O2/16:0 was significantly increased in classic FD patients (Fig. 2D). Among Hex2Cer 18:1;O2 species, peaks at the expected retention time for Ga2 were detectable in some male FD samples, but not consistently across all samples. In platelets, no consistent peaks possibly corresponding to Ga2 were detectable for any of the 17 monitored Hex2Cer species (Fig. S8). Lyso-Hex2Cer 18:1;O2, which includes lyso-Ga2 and lactosylsphingosine (lyso-LacCer) species, was also detected in serum, with significantly higher levels in both, classic ERT-treated and female asymptomatic FD patients (Fig. 2E, Fig. S9A-C). In platelets, lyso-Hex2Cer signals were detectable as well, but showed no significant differences between the groups (Fig. S19). Lyso-Ga2 and lyso-LacCer are isobaric and thus were not distinguishable by the used reversed phase LC-based method.

3.6. Lipidomics profiling of plasma and platelets

We furthermore performed a comprehensive targeted sphingolipidomics analysis, and additionally an analysis of phospholipids, neutral lipids and acylcarnitines using distinct panels. In total, 492 lipid species were quantified in both, platelets and plasma, and additionally 167 species were specific for one of the two matrices (Table S11–S13). We compared the concentrations of different lipid classes and individual lipid species between classic FD and controls (Fig. S13–S15, Table S14–S20). These comparisons revealed significant changes in plasma and platelets within the sphingolipid subclasses and among platelet acylcarnitines.

3.7. Sphingoid base 1-phosphates (S1P) and ganglioside GM3

Total and individual S1P levels were significantly decreased in plasma and serum of FD patients (Fig. 2F, Fig. S10AB). In platelets, total, but not individual, S1P species levels were significantly increased

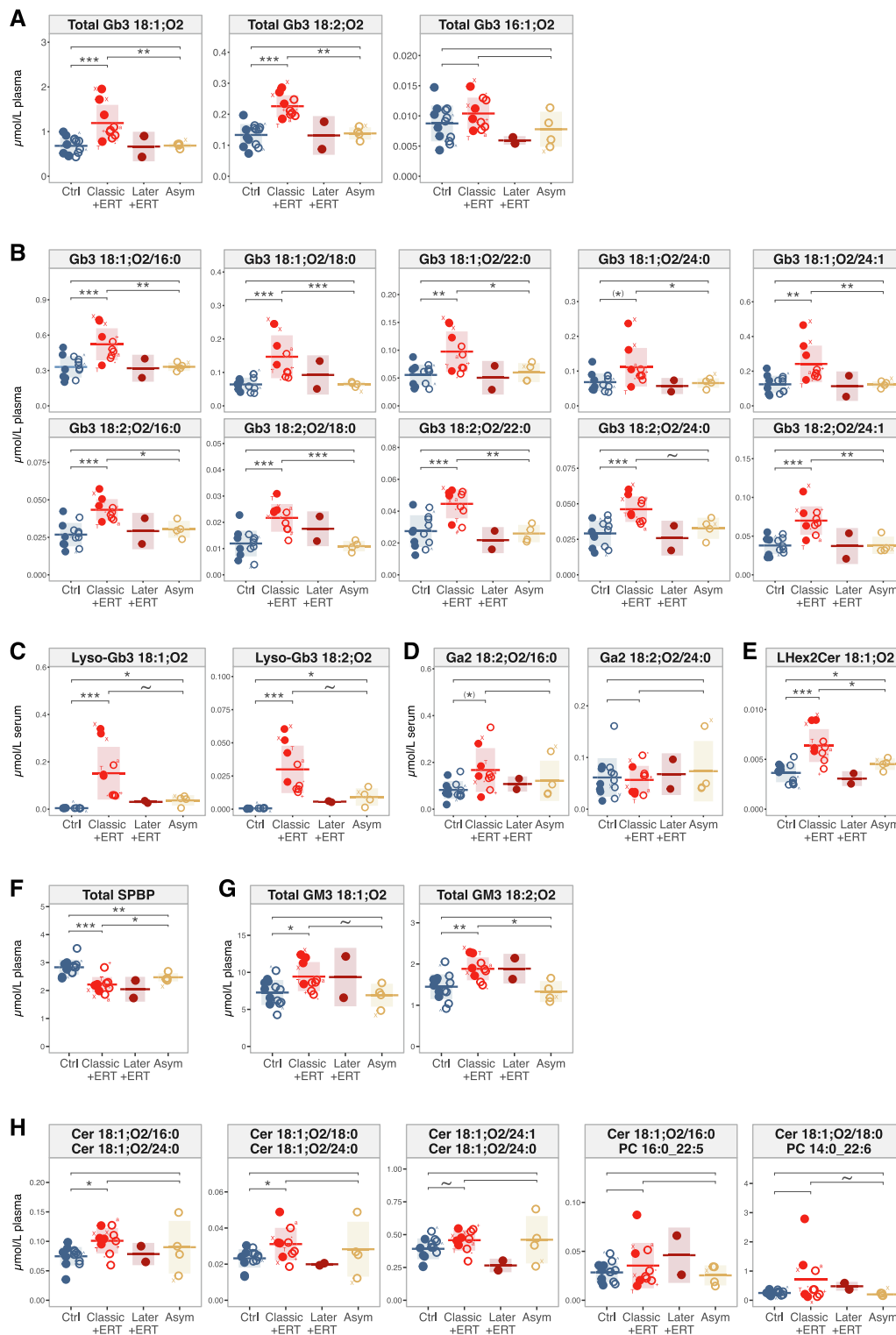


Fig. 2. Plasma and serum lipidome changes in FD. (A) Total concentrations of plasma Gb3 species containing different LCBs. (B) Individual plasma Gb3 species that were significantly increased in any of FD groups. (C) Serum concentrations of the two major lyso-Gb3 species. (D) Serum Ga2 species concentrations. (E) Serum LHex2Cer (which includes lyso-Ga2 and lyso-LacCer) concentrations. (F) Total plasma sphingoid base 1-phosphate concentration. (G) Total concentrations of plasma ganglioside GM3 species with 18:1:O2 and 18:2:O2 LCBS, respectively. (H) Concentration ratios of plasma ceramide species with Cer 18:1:O2/24:0, PC 38:5, or PC 36:6, respectively. Closed and open symbols indicate male and female subjects, respectively. Clas refers to Classic, LaterO/LOn to later-onset, and Asymp/Asy to asymptomatic FD patients. +ERT denotes all patients of the group received enzyme replacement therapy. Vertical bars and shaded boxes depict the mean±SD. Points labelled with X indicate patients with *GLA* frameshift or nonsense mutations, T the patient with a kidney transplant. ^ denotes the two youngest female controls, a, *+, the three oldest female FD patients, see [Table 1](#). *P* value levels: ~ *p* 0.1, **p* ≤ 0.05, ** *p* 0.01, *** *p* 0.001. Significant differences of comparisons with controls had an FDR ≤ 10 %, except those with significant levels in brackets having an FDR of 10–20 %. For the ceramide ratios the FDR was not determined.

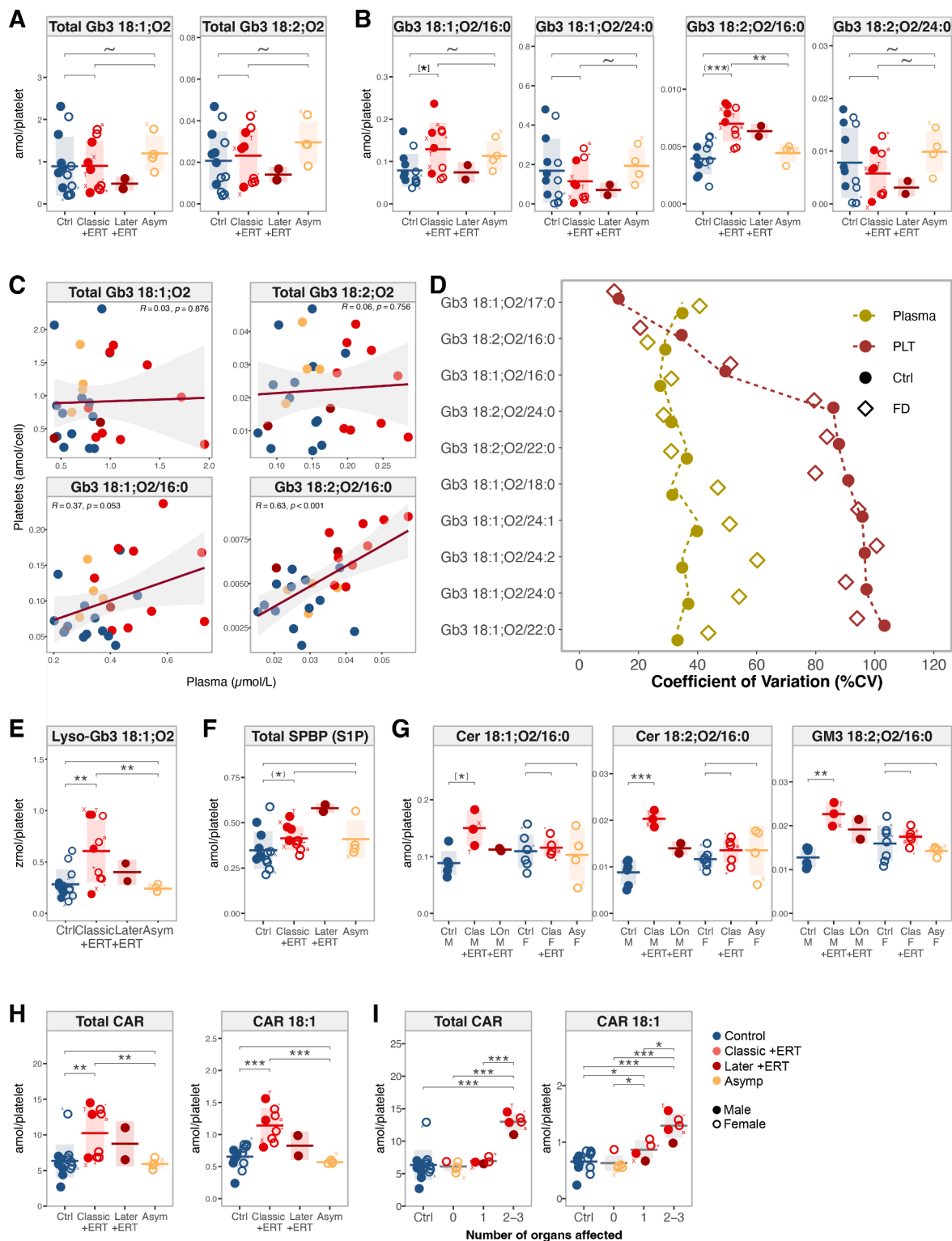


Fig. 3. Platelet lipidome changes in FD. (A) Total concentrations of platelet Gb3 species containing the LCBs 18:1;O2 and 18:2;O2, respectively. (B) Two most abundant LCB 18:1;O2 and 18:2;O2-containing Gb3 species in platelets. (C) Comparison of Gb3 concentrations in platelets with autologous plasma. (D) Between-subject variability Gb3 species in both plasma and platelets from controls and Fabry disease samples, respectively. (E) The only detected lyso-Gb3 species in platelets (F) Total sphingoid base 1-phosphate (S1P). (G) C16:0-containing sphingolipid species. (H) Total long-chain acylcarnitine (LCAR) and the individual long-chain acylcarnitine (CAR) species showing the most significant difference between FD and controls. (I) The same data as in H, but plotted against the number of organs affected in FD patients (see text). Closed and open symbols indicate male and female subjects, respectively. Clas refers to Classic, LaterO/LOn to later-onset, and Asymp/Asy to asymptomatic FD patients. +ERT denotes all patients of the group were received enzyme replacement therapy. Vertical bars and shaded boxes depict the mean±SD. Points labelled with X indicate patients with *GLA* frameshift or nonsense mutations, T the patient with a kidney transplant. ~denotes the two youngest female controls, a,*,+ the three oldest female FD patients, see Table 1. P value levels: ~ p 0.1, * p 0.05, ** p 0.01, *** p 0.001. Significant differences of comparisons with controls had an FDR≤10 %, except those with significant levels in round brackets having an FDR of 10–20 %, and those in square brackets an FDR>20 %.

(Fig. 3F, Fig. S10C). Plasma total levels of the GM3 (monosialodihexosyl-ganglioside) and 7 of 12 GM3 molecular species were significantly increased in FD patients (Fig. 2G and Fig. S10D). However, when sexes were analyzed separately, only male FD patients showed significant increases in GM3 (Fig. S18). In platelets, the molecular species GM3 18:1;O2/20:0 (FDR 40 %) and GM3 18:2;O2/16:0 (FDR 16 %) were significantly increased, but not total GM3 (Fig. S10E and Fig. S19).

3.8. Sphingolipids containing LCB 16:1;O2 and phospholipids containing myristic acid (C14:0)

The plasma total concentrations of ceramide (Cer) and sphingomyelin (SM) species containing the 16:1;O2 LCB were significantly decreased in male classic FD patients (Fig. S11A). At molecular species level, several Cer 16:1;O2 and SM 16:1;O2, in particular those with C22:0 and C24:0 fatty acids, were decreased (Fig. S11C). S1P 16:1;O2, an intermediate of 16:1;O2-sphingolipid degradation [56], was also reduced, which may, however, also be attributed to the reduction of S1P described before. Myristic acid (C14:0-CoA) is the precursor in LCB 16:1;O2 synthesis [57]. We therefore investigated measured phospholipid species that may comprise molecular species with C14:0 (Fig. S11BD). LPC 14:0 and PC 28:0 (comprising PC 14:0_14:0) had significantly lower levels in male FD patients, albeit with FDRs > 70%. In platelets, no significant differences in LCB 16:1;O2-containing sphingolipids and C14:0-containing phospholipids were present between the groups (Fig. S22).

3.9. Ceramide ratios

Since cardiovascular manifestations in FD are frequent, we explored specific plasma ceramide concentrations ratios used in the Coronary Event Risk Tests (CERT1/2) [58]. In classic FD patients, the ratios [Cer 18:1;O2/16:0]/[Cer 18:1;O2/24:0] and [Cer 18:1;O2/18:0]/[Cer 18:1;O2/24:0] were significantly increased (Fig. 2H). Two male classic FD patients had higher values in 4 of the 5 tested ratios compared to any of the male control participants. In particular, the [Cer 18:1;O2/18:0]/[PC 14:0_22:6] ratio was 5 to 12-fold higher compared to the average of controls. These 2 patients had no cardiac manifestation, as assessed by LMMVI, but impaired kidney function (Table 1). The later-onset FD patient with a cardiac variant had elevated ratios of [Cer 18:1;O2/16:0]/[PC 14:0_22:6] and [Cer 18:1;O2/18:0]/[PC 16:0_22:5]. The oldest female FD patient had a highly increased LVMMI and impaired kidney function (Table 1), as well as higher [Cer 18:1;O2/18:0]/[PC 14:0_22:6], [Cer 18:1;O2/16:0]/[Cer 18:1;O2/24:0] and [Cer 18:1;O2/18:0]/[Cer 18:1;O2/24:0] ratios compared to any of the control subjects (Fig. 2H).

3.10. C16:0-containing ceramides

In platelets, the C16:0-containing Cer 18:2;O2/16:0, SM 18:2;O2/16:0, and Gb4 18:2;O2/16:0 were significantly increased in male classic FD patients (Fig. 3G, Fig. S12A). Gb3 18:1;O2/16:0, Gb3 18:2;O2/16:0, and GM3 18:2;O2/16:0 were also significantly increased, as described before. Some additional platelet 18:2;O2/16:0 containing species were also increased, albeit with FDRs > 10 %, while in plasma, no significant increases of C16:0-containing ceramide and sphingomyelin species were observed (Table S18-S20).

3.11. Long-chain acylcarnitines

Total levels of long-chain acylcarnitines (LCAR) were calculated from 16 measured CAR species with chain lengths of C12–C18. Total LCAR was significantly increased in classic FD patients (Fig. 3H). When relating the number of organ systems affected in the patients, i.e., with renal, cardiovascular or neurological involvement (Table 1), total LCAR levels were distinctly higher when 2 or more organ systems were

affected, independent of the FD disease group (Fig. 3I). CAR 18:1 showed the most significant change among the 11 increased LCAR species and also displayed a significant dependence with number of organs affected, as all the other 15 CAR species (Fig. 3HI and Fig. S12BC). One female control subject had distinctly higher levels of total LCAR, and of most individual LCAR species, however her CAR 18:1 levels were within the range of the other controls (Fig. S12BC).

3.12. Phosphoglycerolipids and neutral lipids

In plasma, no significant differences in the phosphoglycerolipid and neutral lipid classes were identified (Fig. S14–S15). In platelets, total LPE, PG and PI was significantly increased, but at species level no significant differences were present (Table S14, S15, S18–S20).

4. Discussion

We used a targeted lipidomics approach to identify potential new FD markers, and changes in plasma and platelet lipidomes beyond Gb3 and its metabolites. The statistical analysis focused on samples from ERT-treated symptomatic, male and female, classic FD patients, and corresponding healthy individuals. The two male later-onset and the untreated asymptomatic female FD patients were included in the discussions when potential changes in these groups were observed.

Gb3 in the context of FD is commonly reported as concentration of total Gb3, determined from the sum of species harboring the LCB sphingosine (18:1;O2). So far, only Manwaring et al. [59] reported two plasma sphingadiene (18:2;O2)-containing Gb3 species to be elevated in FD. We found that total and individual plasma levels of both Gb3 18:1;O2 and Gb3 18:2;O2 species were also significantly increased in male and female, ERT-treated, classic FD patients. Gb3 18:2;O2 concentrations showed more significant differences between controls and FD compared to Gb3 18:1;O2, especially in female FD patients. Our results hence extend findings by Manwaring et al. [59] by identifying that the majority of the measured 18:2;O2-containing Gb3 species are increased in ERT-treated FD patients. Future studies in different cohorts comparing with the typically measured total Gb3 and lyso-Gb3 levels would help to understand the utility of these Gb3 18:2;O2 species in FD screening.

Serum lyso-Gb3 species were distinctly elevated in ERT-treated FD patients, consistent with the existing literature [16,60]. Lyso-Gb3 was also increased in asymptomatic female classic FD patients, unlike Gb3 in this study. Galabiosylceramides (Ga2, Fig. 1B) were shown to accumulate in kidneys and urine in FD [34,61]. However, only Vance et al. [62] reported the possible presence of Ga2 in plasma from FD patients. We were able to detect and quantify 2 Ga2 species in serum, interestingly, both of which comprised the LCB 18:2;O2. One of them, Ga2 18:2;O2/16:0, was significantly elevated in classic ERT-treated FD patients. This represents another example of an 18:2;O2/16:0 sphingolipid species increased in FD in this study. Furthermore, lyso-Hex2Cer (also referred to as lyso-CDH), which includes the structural isomers lyso-Ga2 and lactosylsphingosine, was also increased in classic ERT-treated FD patients. To our knowledge, lyso-Hex2Cer has so far only been shown to be increased in dried blood spots in context of FD [63]. Serum lyso-Hex2Cer can be measured together with lyso-Gb3 in the same LC-MS analysis, as it was done in this study. It would be interesting to include this lipid species in lyso-Gb3 analyses of future studies to evaluate its value in FD diagnosis and monitoring.

Many of the lipid species identified in this study are already, or can be, included in LC-MS methods used for large lipidomics studies [36,38]. Analysis of these lipid species in clinical and population studies may provide new insights into possible FD prevalence in different populations, without the need for dedicated screenings.

Platelet total Gb3 levels were not increased in FD patients in our study. The ERT may therefore be effective in preventing Gb3 accumulation in human platelets. In a FD rat model, platelets and red blood cells

(RBC) accumulated Gb3, but this was not the case for RBCs of untreated FD patients [62,64,65]. No conclusions can be made based on this background for the absence of Gb3 accumulation in platelets, as there were no untreated FD patients included in this study. However, lyso-Gb3 was significantly elevated in platelet of FD patients, indicating a possible transient accumulation of Gb3 and a potential involvement of platelets in FD even under ERT.

The molecular species Gb3 18:2;O2/16:0 was however significantly increased in FD platelets. Furthermore, this species had a distinctly lower inter-individual variability in platelets and was the only one exhibiting a significant correlation with corresponding levels in plasma. Other sphingolipid species comprising 18:2;O2/16:0, i.e., Cer, SM, Gb4, and GM3, were also significantly increased in platelets of FD patients. Mechanisms other than reduced GLA activity may have contributed to these distinct changes of these lipid species.

We observed a high inter-individual variability of very long-chain Gb3 species in platelets, which may also have masked differences in Gb3 between the groups. A distinct inter-individual variability of total Gb3 (also termed *Pk* antigen) in human platelets has been reported previously [66], whereas no data are available on individual Gb3 species. In RBCs, Gb3 was shown to correlate with the P1PK blood group antigen P1, which has a high inter-individual variability and is also present in platelets [67–69]. Gb3 and P1 are both products of the alpha 1,4-galactosyl-transferase A4GALT (Fig. 1), of which the transcriptional regulation in different P1PK P¹/P² genotypes were suggested to partially define P1 and consequently Gb3 levels [68]. In human macrophages, very long-chain Gb3 species also exhibited a high inter-individual variability [70]. The clinical relevance of this very-long chain Gb3 variability in FD and other conditions is yet to be explored.

We observed increased plasma concentrations of the ganglioside GM3 in classic FD patients. No published data on plasma GM3 in human FD were available from the literature. The observed GM3 increase might be the result of increased availability of its substrate LacCer (Fig. 1B), perhaps as a result from an increased local or temporal breakdown of accumulated Gb3 resulting from ERT. A link between elevated plasma GM3 and Parkinson is being discussed [71,72], and an increased incidence of Parkinson's disease has been observed in FD [73,74]. A verification of these data in larger cohorts may be valuable, due to the novelty and the potential implications of this result.

Plasma and serum total S1P were significantly lower in ERT-treated FD patients in our study. In contrast, a previous study reported increased plasma S1P levels in untreated FD patients [75]. This discrepancy may be attributed to that patients in our study were under ERT, however, the untreated asymptomatic female patients also had lower plasma S1P levels. Important for the interpretation of these results is that plasma samples were obtained from whole blood that was stored 2–4 h at room temperature, which was shown to considerably increase S1P levels *ex vivo* [76,77]. Lower plasma or serum S1P levels in FD may be the result of an impaired *ex vivo* release of S1P from RBCs [78,79]. Consistent with previous reports [80], male FD patients had significantly lower hematocrit, which is known to be associated with S1P levels [78,81]. Female patients, however, had normal hematocrit but still reduced S1P levels in our study. S1P has diverse functions [82], and e.g., reduced serum S1P levels have been associated with severity of stroke, a possible symptom of FD [83–85]. While these data on S1P must be confirmed with appropriate pre-analytics in larger cohorts, this lipid mediator class may represent an interesting supporting diagnostic and prognostic marker in FD.

Plasma levels of several sphingolipids containing the LCB 16:1;O2 and phospholipids harboring myristic acid (C14:0), were reduced in male ERT-treated FD patients. C14:0-CoA is a precursor of LCB 16:1;O2 synthesis [57]. These findings suggest a potential reduction of the plasma C14:0 pool in male FD patients. While gastrointestinal manifestations in FD that can lead to changes in the gut microbiome and food absorption [86,87], the actual mechanisms and relevance of our observation remains to be elucidated.

Classic FD patients had increased plasma ceramide C16:0/C24:0 and C18:0/C24:0 ratios, which are associated with risk for cardiovascular disease (CVD) and are components of the CERT1 score [58,88–90]. Other ceramide-based ratios of the CERT1/CERT2 scores were also increased in certain patients [91]. Two FD patients had LVH, and half had impaired kidney function and elevated NT-proBNP, indicating frequent cardiac complications such as myocardial edema and injury [92]. The presence of the cardio-renal syndrome (CRS) is further associated with a markedly increased CVD risk [93]. While our sample size was insufficient to calculate CERT1/2 scores, our findings suggest a potential utility of such risk scores in prognosis and monitoring of cardiac manifestations in FD.

Platelet lyso-Gb3 levels were increased in FD patients, suggesting an implication of FD on platelets. Long-chain acylcarnitines (LCAR) were elevated in FD patients' platelets, especially when two or more organs were impaired, suggesting a possible association of platelet LCARs with FD disease severity. Accumulation of LCARs in stored platelets have been implicated in reduced platelet lifespan and mitochondrial damage [94]. Platelets from male FD patients also had increased levels C16:0-harboring sphingolipids, which are implicated in stress response and apoptosis [90,95–97]. Increased platelet levels of C16:0-ceramide and LCAR species have been reported in patients with symptomatic coronary artery disease [98]. Furthermore, platelet S1P levels were also increased in FD. Increased intracellular S1P synthesis as response to cellular stress leading to pro-inflammatory events has been shown for human dermal fibroblasts [99]. Taken together, these findings may be reflective of cellular stress and mitochondrial dysfunction that occur in platelets in FD. Whether these changes are the consequence of the prothrombotic state seen in FD [24,25] or other mechanisms, and their clinical relevance remains to be elucidated.

We found no significant differences in plasma phospholipids and neutral lipids between FD and control groups, which contrasts with a published metabolomics study of a cohort comprising untreated and ERT-treated FD patients [100]. This may be explained by differences in the sample sizes, in the cohorts, and possibly also by the different origin and pre-analytics of control and FD samples [28,100].

Limitations of this study include the small sample size resulting in limited statistical power and risk for sampling bias (see power calculation Fig. S20). The female control participants were considerably younger than the female FD patients. Plasma Gb3, GM3 and Cer were shown to be positively associated with age by estimated 0.1–0.4 % per year [101], thus the age difference may have partially contributed to the observed effects. However, all observed differences were also present in male patients, which had comparable ages as their corresponding controls. Another limitation is that all symptomatic FD patients have received ERT for two or more years. This limitation affects conclusions regarding untreated FD patients, but it also reflects the status of many FD patients. To harmonize and minimize short-term effects of the ERT, samples were taken immediately before the bi-weekly ERT infusion, whereby patients were not fasted. While the fasting state was shown to have some effect on the levels of specific circulating sphingolipid species [102], both, the healthy participants and FD patients were non-fasted in this study.

In conclusion, this study revealed plasma and platelet lipidome changes in ERT-treated FD patients that extend beyond Gb3 and its metabolites. These findings may add new aspects in the understanding of the systemic lipid metabolism in FD disease. Furthermore, this study identified sphingadiene (18:2;O2)-containing Gb3, lyso-Hex2Cer, and possibly, S1P, GM3, and ceramide ratios, as potential new markers for screening, prognosis, and treatment monitoring of FD patients. Further studies in larger and different FD cohorts will allow to validate and extend the findings of this study.

Funding information

This work was supported by an Investigator Initiated Research Grant [no. IISR-2014-104023 / IIR-CHE-000372] from Shire International GmbH, a Takeda company. Work of B.B., J.O., F.T., D.M., A.K.B. and M.

R.W. was supported by grants from the National University of Singapore via the Life Sciences Institute (LSI); the National Research Foundation Singapore [NRFSBP-P4], and Agency for Science, Technology and Research A*STAR [IAF-ICP I1901E0040].

CRedit authorship contribution statement

Bo Burla: Writing – review & editing, Writing – original draft, Visualization, Supervision, Software, Project administration, Methodology, Investigation, Formal analysis, Data curation, Conceptualization. **Jeongah Oh:** Writing – review & editing, Methodology, Investigation, Data curation, Conceptualization. **Albina Nowak:** Writing – review & editing, Supervision, Resources, Data curation, Conceptualization. **Nathalie Piraud:** Resources, Investigation. **Eduardo Meyer:** Methodology. **Ding Mei:** Investigation. **Anne K. Bendt:** Writing – review & editing, Project administration. **Jan-Dirk Studt:** Resources, Methodology, Conceptualization. **Beat M. Frey:** Writing – review & editing, Resources, Methodology. **Federico Torta:** Conceptualization, Methodology, Writing - Original Draft, Writing - Review & Editing. **Markus R. Wenk:** Writing – original draft, Resources, Conceptualization. **Pierre-Alexandre Krayenbuehl:** Writing – original draft, Visualization, Supervision, Resources, Project administration, Funding acquisition, Formal analysis, Data curation, Conceptualization.

Declaration of Competing Interest

The authors declare that they have no known competing financial interests or personal relationships that could have appeared to influence the work reported in this paper.

Acknowledgements

We thank HTHC High Tech Home Care AG, Rotkreuz, Switzerland, for collecting the samples, and Petra Noordmans and team, Linth Hospital Uznach, Switzerland, for performing blood tests.

Data availability

The Lipidomics Minimal Reporting checklist is available from the [supplementary materials](#) and via DOI: [10.5281/zenodo.12627121](https://doi.org/10.5281/zenodo.12627121). The lipidomics datasets with MS raw data, and the archived GitHub repository with the R pipeline and metadata have been deposited in Zenodo (DOI: [10.5281/zenodo.11634068](https://doi.org/10.5281/zenodo.11634068)). The Github repository can be accessed at https://github.com/SLINGhub/Burla_2024_FabryLipidomics.

Appendix A. Supplementary data

Supplementary data to this article can be found online at <https://doi.org/10.1016/j.cca.2024.119833>.

References

- [1] D.P. Germain, Fabry disease, *Orphanet J. Rare Dis.* 5 (2010) 30, <https://doi.org/10.1186/1750-1172-5-30>.
- [2] D.P. Germain, G. Altarescu, R. Barria-Villa, R. Mignani, K. Pawlaczyk, F. Pieruzzi, W. Terryn, B. Vujkovic, A. Ortiz, An expert consensus on practical clinical recommendations and guidance for patients with classic Fabry disease, *Mol. Genet. Metab.* 137 (2022) 49–61, <https://doi.org/10.1016/j.ymgme.2022.07.010>.
- [3] A. Ortiz, D.P. Germain, R.J. Desnick, J. Politei, M. Mauer, A. Burlina, C. Eng, R. J. Hopkin, D. Laney, A. Linhart, S. Waldek, E. Wallace, F. Weidemann, W. R. Wilcox, Fabry disease revisited: Management and treatment recommendations for adult patients, *Mol. Genet. Metab.* 123 (2018) 416–427, <https://doi.org/10.1016/j.ymgme.2018.02.014>.
- [4] P. Elliott, R. Baker, F. Pasquale, G. Quarta, H. Ebrahim, A.B. Mehta, D.A. Hughes, Prevalence of Anderson-Fabry disease in patients with hypertrophic cardiomyopathy: the European Anderson-Fabry Disease Survey, *Heart* 97 (2011) 1957–1960, <https://doi.org/10.1136/heartjnl-2011-300364>.
- [5] M.J. Hilz, E. Arbustini, L. Dagna, A. Gasbarrini, C. Goizet, D. Lacombe, R. Liguori, R. Manna, J. Politei, M. Spada, A. Burlina, Non-specific gastrointestinal features: Could it be Fabry disease? *Dig. Liver Dis.* 50 (2018) 429–437, <https://doi.org/10.1016/j.dld.2018.02.011>.
- [6] A. Mallett, P.J. Kearey, A. Cameron, H.G. Healy, C. Denaro, M. Thomas, V.W. Lee, S.L. Stark, M. Fuller, Z. Wang, W.E. Hoy, The prevalence of Fabry disease in a statewide chronic kidney disease cohort – Outcomes of the aCQuiRE (Ckd.Qld fabry Epidemiology) study, *BMC Nephrol.* 23 (2022) 169, <https://doi.org/10.1186/s12882-022-02805-8>.
- [7] Q. Shi, J. Chen, J. Pongmoragot, S. Lanthier, G. Saposnik, Prevalence of Fabry Disease in Stroke Patients—A Systematic Review and Meta-analysis, *J. Stroke Cerebrovasc. Dis.* 23 (2014) 985–992, <https://doi.org/10.1016/j.jstrokecerebrovasdis.2013.08.010>.
- [8] M. Gilchrist, F. Casanova, J.S. Tyrrell, S. Cannon, A.R. Wood, N. Fife, K. Young, R. A. Oram, M.N. Weedon, Prevalence of Fabry disease-causing variants in the UK Biobank, *J. Med. Genet.* (2022), <https://doi.org/10.1136/jmg-2022-108523>.
- [9] X. Li, X. Ren, Y. Zhang, L. Ding, M. Huo, Q. Li, Fabry disease: Mechanism and therapeutics strategies, accessed March 13, 2023, *Front. Pharmacol.* 13 (2022), <https://www.frontiersin.org/articles/10.3389/fphar.2022.1025740>.
- [10] M.A. Hölzl, M. Gärtner, J.J. Kovarik, J. Hofer, H. Bernheimer, G. Sunderplasmann, G.J. Zlabinger, Quantification of α -galactosidase activity in intact leukocytes, *Clin. Chim. Acta* 411 (2010) 1666–1670, <https://doi.org/10.1016/j.cca.2010.06.023>.
- [11] A.M. Martins, V. D'Almeida, S.O. Kyosen, E.T. Takata, A.G. Delgado, Á.M.B. F. Gonçalves, C.C.B. Filho, D.M. Filho, G. Biagini, H. Pimentel, H. Abensur, H. C. Guimarães, J.G. Gomes, J.S. Neto, L.O.D. D'Almeida, L.R. Carvalho, M. B. Harouche, M.C.J. Maldonado, O.J.M. Nascimento, P.S. dos S. Montoril, R. V. Bastos, Guidelines to Diagnosis and Monitoring of Fabry Disease and Review of Treatment Experiences, *J. Pediatr.* 155 (2009) S19–S31, <https://doi.org/10.1016/j.jpeds.2009.07.003>.
- [12] R. Schiffmann, M. Fuller, L.A. Clarke, J.M.F.G. Aerts, Is it Fabry disease? *Genet. Med.* 18 (2016) 1181–1185, <https://doi.org/10.1038/gim.2016.55>.
- [13] A.R. Stiles, H. Zhang, J. Dai, P. McCaw, J. Beasley, C. Rehder, D.D. Koeberl, M. McDonald, D.S. Bali, S.P. Young, A comprehensive testing algorithm for the diagnosis of Fabry disease in males and females, *Mol. Genet. Metab.* 130 (2020) 209–214, <https://doi.org/10.1016/j.ymgme.2020.04.006>.
- [14] J.M. Aerts, J.E. Groener, S. Kuiper, W.E. Donker-Koopman, A. Strijland, R. Ottenhoff, C. van Roomen, M. Mirzaian, F.A. Wijburg, G.E. Linthorst, A. C. Vedder, S.M. Rombach, J. Cox-Brinkman, P. Somerharju, R.G. Boot, C. E. Hollak, R.O. Brady, B.J. Poorthuis, Elevated globotriaosylsphingosine is a hallmark of Fabry disease, *Proc. Natl. Acad. Sci.* 105 (2008) 2812–2817, <https://doi.org/10.1073/pnas.0712309105>.
- [15] H. Maruyama, K. Miyata, M. Mikame, A. Taguchi, C. Guili, M. Shimura, K. Murayama, T. Inoue, S. Yamamoto, K. Sugimura, K. Tamita, T. Kawasaki, J. Kajihara, A. Onishi, H. Sugiyama, T. Sakai, I. Murata, T. Oda, S. Toyoda, K. Hanawa, T. Fujimura, S. Ura, M. Matsumura, H. Takano, S. Yamashita, G. Matsukura, R. Tazawa, T. Shiga, M. Ebato, H. Satoh, S. Ishii, Effectiveness of plasma lyso-Gb3 as a biomarker for selecting high-risk patients with Fabry disease from multispecialty clinics for genetic analysis, *Genet. Med.* 21 (2019) 44–52, <https://doi.org/10.1038/gim.2018.31>.
- [16] A. Nowak, T.P. Mechtler, T. Hornemann, J. Gawinecka, E. Theswet, M.J. Hilz, D. C. Kasper, Genotype, phenotype and disease severity reflected by serum LysoGb3 levels in patients with Fabry disease, *Mol. Genet. Metab.* 123 (2018) 148–153, <https://doi.org/10.1016/j.ymgme.2017.07.002>.
- [17] A. Nowak, F. Beuschlein, V. Sivasubramaniam, D. Kasper, D.G. Warnock, Lyso-Gb3 associates with adverse long-term outcome in patients with Fabry disease, *J. Med. Genet.* 59 (2022) 287–293, <https://doi.org/10.1136/jmedgenet-2020-107338>.
- [18] R. Krüger, K. Bruns, S. Grünhage, H. Rossmann, J. Reinke, M. Beck, K.J. Lackner, Determination of globotriaosylceramide in plasma and urine by mass spectrometry, *Clin. Chem. Lab. Med.* 48 (2010) 189–198, <https://doi.org/10.1515/CCLM.2010.048>.
- [19] B.C. Nelson, T. Roddy, S. Araghi, D. Wilkens, J.J. Thomas, K. Zhang, C.-C. Sung, S.M. Richards, Globotriaosylceramide isoform profiles in human plasma by liquid chromatography–tandem mass spectrometry, *J. Chromatogr. B* 805 (2004) 127–134, <https://doi.org/10.1016/j.jchromb.2004.02.032>.
- [20] T.P. Roddy, B.C. Nelson, C.C. Sung, S. Araghi, D. Wilkens, X.K. Zhang, J. J. Thomas, S.M. Richards, Liquid Chromatography–Tandem Mass Spectrometry Quantification of Globotriaosylceramide in Plasma for Long-Term Monitoring of Fabry Patients Treated with Enzyme Replacement Therapy, *Clin. Chem.* 51 (2005) 237–240, <https://doi.org/10.1373/clinchem.2004.038323>.
- [21] S. Jabbarzadeh-Tabrizi, M. Boutin, T.S. Day, M. Taroua, R. Schiffmann, C. Auray-Blais, J.-S. Shen, Assessing the role of glycosphingolipids in the phenotype severity of Fabry disease mouse model, *J. Lipid Res.* 61 (2020) 1410–1423, <https://doi.org/10.1194/jlr.RA12000909>.
- [22] A. Taguchi, S. Ishii, M. Mikame, H. Maruyama, Distinctive accumulation of globotriaosylceramide and globotriaosylsphingosine in a mouse model of classic Fabry disease, *Mol. Genet. Metab. Rep.* 34 (2023) 100952, <https://doi.org/10.1016/j.ymgmr.2022.100952>.
- [23] T. DeGraba, S. Azhar, F. Dignat-George, E. Brown, B. Bouët, G. Altarescu, R. McCarron, R. Schiffmann, Profile of endothelial and leukocyte activation in fabry patients, *Ann. Neurol.* 47 (2000) 229–233, [https://doi.org/10.1002/1531-8249\(200002\)47:2<229::AID-ANA13>3.0.CO;2-T](https://doi.org/10.1002/1531-8249(200002)47:2<229::AID-ANA13>3.0.CO;2-T).
- [24] T. Igarashi, H. Sakuraba, Y. Suzuki, Activation of platelet function in Fabry's disease, *Am. J. Hematol.* 22 (1986) 63–67, <https://doi.org/10.1002/ajh.2830220110>.

- [25] A.C. Vedder, É. Biró, J.M.F.G. Aerts, R. Nieuwland, G. Sturk, C.E.M. Hollak, Plasma markers of coagulation and endothelial activation in Fabry disease: impact of renal impairment, *Nephrol. Dial. Transplant.* (2009) gfp263, <https://doi.org/10.1093/ndt/gfp263>.
- [26] K. Ahluwalia, B. Ebright, K. Chow, P. Dave, A. Mead, R. Poblete, S.G. Louie, I. Asante, Lipidomics in Understanding Pathophysiology and Pharmacologic Effects in Inflammatory Diseases: Considerations for Drug Development, *Metabolites* 12 (2022) 333, <https://doi.org/10.3390/metabo12040333>.
- [27] F. Yan, Z. Wen, R. Wang, W. Luo, Y. Du, W. Wang, X. Chen, Identification of the lipid biomarkers from plasma in idiopathic pulmonary fibrosis by Lipidomics, *BMC Pulm. Med.* 17 (2017) 174, <https://doi.org/10.1186/s12890-017-0513-4>.
- [28] Q. Wang, M. Hoene, C. Hu, L. Fritsche, R. Ahrends, G. Liebisch, K. Ekroos, A. Fritsche, A.L. Birkenfeld, X. Liu, X. Zhao, Q. Li, B. Su, A. Peter, G. Xu, R. Lehmann, Ex vivo instability of lipids in whole blood: preanalytical recommendations for clinical lipidomics studies, *J. Lipid Res.* 64 (2023), <https://doi.org/10.1016/j.jlr.2023.100378>.
- [29] C. Delgado, M. Baweja, D.C. Crews, N.D. Eneanya, C.A. Gadegbeku, L.A. Inker, M. L. Mendu, W.G. Miller, M.M. Moxey-Mims, G.V. Roberts, W.L.S. Peter, C. Warfield, N.R. Powe, A. Unifying Approach for GFR Estimation: Recommendations of the NKF-ASN Task Force on Reassessing the Inclusion of Race in Diagnosing Kidney Disease, *Am. J. Kidney Dis.* 79 (2022) 268–288.e1, <https://doi.org/10.1053/j.ajkd.2021.08.003>.
- [30] J.M. Burkhart, M. Vaudel, S. Gambaryan, S. Radau, U. Walter, L. Martens, J. Geiger, A. Sickmann, R.P. Zahedi, The first comprehensive and quantitative analysis of human platelet protein composition allows the comparative analysis of structural and functional pathways, *Blood* 120 (2012) e73–e82, <https://doi.org/10.1182/blood-2012-04-416594>.
- [31] M. Yokota, N. Tatsumi, I. Tsuda, T. Nishioka, T. Takubo, CTAD as a universal anticoagulant, *J. Anal. Methods Chem.* 25 (2003) 17–20, <https://doi.org/10.1155/S1463924603000038>.
- [32] Z.H. Alshehry, C.K. Barlow, J.M. Weir, Y. Zhou, M.J. McConville, P.J. Meikle, An efficient single phase method for the extraction of plasma lipids, *Metabolites* 5 (2015) 389–403, <https://doi.org/10.3390/metabo5020389>.
- [33] J. Beasley, P. McCaw, H. Zhang, S.P. Young, A.R. Stiles, Combined analysis of plasma or serum glucosylsphingosine and globotriaosylsphingosine by UPLC-MS/MS, *Clin. Chim. Acta* 511 (2020) 132–137, <https://doi.org/10.1016/j.cca.2020.10.007>.
- [34] M. Boutin, I. Menkovic, T. Martineau, V. Vaillancourt-Lavigne, A. Toupin, C. Auray-Blais, Separation and Analysis of Lactosylceramide, Galabiosylceramide, and Globotriaosylceramide by LC-MS/MS in Urine of Fabry Disease Patients, *Anal. Chem.* 89 (2017) 13382–13390, <https://doi.org/10.1021/acs.analchem.7b03609>.
- [35] S. Muralidharan, M. Shimobayashi, S. Ji, B. Burla, M.N. Hall, M.R. Wenk, F. Torta, A reference map of sphingolipids in murine tissues, *Cell Rep.* 35 (2021) 109250, <https://doi.org/10.1016/j.celrep.2021.109250>.
- [36] B. Burla, S. Muralidharan, M.R. Wenk, F. Torta, Sphingolipid Analysis in Clinical Research, *Methods Mol. Biol.* (2018), https://doi.org/10.1007/978-1-4939-7592-1_11.
- [37] P. Narayanaswamy, S. Shinde, R. Sulc, R. Kraut, G. Staples, C.H. Thiam, R. Grimm, B. Sellergren, F. Torta, M.R. Wenk, Lipidomic “deep profiling”: an enhanced workflow to reveal new molecular species of signaling lipids, *Anal. Chem.* 86 (2014) 3043–3047, <https://doi.org/10.1021/ac4039652>.
- [38] K. Huynh, C.K. Barlow, K.S. Jayawardana, J.M. Weir, N.A. Mellett, M. Cinel, D. J. Magliano, J.E. Shaw, B.G. Drew, P.J. Meikle, High-Throughput Plasma Lipidomics: Detailed Mapping of the Associations with Cardiometabolic Risk Factors, *Cell, Chem. Biol.* 26 (2019) 71–84.e4, <https://doi.org/10.1016/j.chembiol.2018.10.008>.
- [39] Baker Heart and Diabetes Institute Metabolomics Laboratory Portal, (2023). <https://metabolomics.baker.edu.au/method/lipids>.
- [40] L. Gao, S. Ji, B. Burla, M.R. Wenk, F. Torta, A. Cazenave-Gassiot, LICAR: An Application for Isotopic Correction of Targeted Lipidomic Data Acquired with Class-Based Chromatographic Separations Using Multiple Reaction Monitoring, *Anal. Chem.* 93 (2021) 3163–3171, <https://doi.org/10.1021/acs.analchem.0c04565>.
- [41] W.B. Dunn, D. Broadhurst, P. Begley, E. Zelena, S. Francis-McIntyre, N. Anderson, M. Brown, J.D. Knowles, A. Halsall, J.N. Haselden, A.W. Nicholls, I.D. Wilson, D. B. Kell, R. Goodacre, Procedures for large-scale metabolic profiling of serum and plasma using gas chromatography and liquid chromatography coupled to mass spectrometry, *Nat. Protoc.* 6 (2011) 1060–1083, <https://doi.org/10.1038/nprot.2011.335>.
- [42] F. Hildebrand, H. Schoeny, E. Rampler, G. Koellensperger, Scrutinizing different ionization responses of polar lipids in a reversed-phase gradient by implementing a counter-gradient, *Anal. Chim. Acta* 1265 (2023) 341274, <https://doi.org/10.1016/j.aca.2023.341274>.
- [43] G. Liebisch, E. Fahy, J. Aoki, E.A. Dennis, T. Durand, C.S. Ejsing, M. Fedorova, I. Feussner, W.J. Griffiths, H. Köfeler, A.H. Merrill, R.C. Murphy, V.B. O'Donnell, O. Oskolkova, S. Subramaniam, M.J.O. Wakelam, F. Spener, Update on LIPID MAPS classification, nomenclature, and shorthand notation for MS-derived lipid structures, *J. Lipid Res.* 61 (2020) 1539–1555, <https://doi.org/10.1194/jlr.S120001025>.
- [44] J.G. McDonald, C.S. Ejsing, D. Kocpczynski, M. Holcapek, J. Aoki, M. Arita, M. Arita, E.S. Baker, J. Bertrand-Michel, J.A. Bowden, B. Brügger, S.R. Ellis, M. Fedorova, W.J. Griffiths, X. Han, J. Hartler, N. Hoffmann, J.P. Koelmel, H. C. Köfeler, T.W. Mitchell, V.B. O'Donnell, D. Saigusa, D. Schwudke, A. Shevchenko, C.Z. Ulmer, M.R. Wenk, M. Witting, D. Wolrab, Y. Xia, R. Ahrends, G. Liebisch, K. Ekroos, Introducing the Lipidomics Minimal Reporting Checklist, *Nat. Metab.* 4 (2022) 1086–1088, <https://doi.org/10.1038/s42255-022-00628-3>.
- [45] Y. Benjamini, Y. Hochberg, Controlling the false discovery rate: A practical and powerful approach to multiple testing, *J. R. Stat. Soc. Ser. B Methodol.* 57 (1995) 289–300, <https://doi.org/10.1111/j.2517-6161.1995.tb02031.x>.
- [46] J.D. Storey, A direct approach to false discovery rates, *J. R. Stat. Soc. Ser. B Stat. Methodol.* 64 (2002) 479–498, <https://doi.org/10.1111/1467-9868.00346>.
- [47] C. Ahlmann-Eltze, I. Patil, ggsignif: R Package for Displaying Significance Brackets for “ggplot2,” (2021). Doi: 10.31234/osf.io/7awm6.
- [48] R. Iannone, J. Cheng, B. Schloerke, E. Hughes, A. Lauer, J. Seo, gt: Easily create presentation-ready display tables, 2023. <https://CRAN.R-project.org/package=gt>.
- [49] A. Kassambara, ggpubr: “ggplot2” based publication ready plots, 2023. <https://CRAN.R-project.org/package=ggpubr>.
- [50] T.L. Pedersen, patchwork: The composer of plots, 2022. <https://CRAN.R-project.org/package=patchwork>.
- [51] H. Wickham, M. Averick, J. Bryan, W. Chang, L.D. McGowan, R. François, G. Grolemund, A. Hayes, L. Henry, J. Hester, M. Kuhn, T.L. Pedersen, E. Miller, S. M. Bach, K. Müller, J. Ooms, D. Robinson, D.P. Seidel, V. Spinu, K. Takahashi, D. Vaughan, C. Wilke, K. Woo, H. Yutani, Welcome to the Tidyverse, *J. Open Source Softw.* 4 (2019) 1686, <https://doi.org/10.21105/joss.01686>.
- [52] J.D. Storey, A.J. Bass, A. Dabney, D. Robinson, qvalue: Q-value estimation for false discovery rate control, 2023. Doi: 10.18129/B9.bioc.qvalue.
- [53] D.P. Germain, E. Brand, A. Burlina, F. Cecchi, S.C. Garman, J. Kempf, D.A. Laney, A. Linhart, L. Marodi, K. Nicholls, A. Ortiz, F. Pieruzzi, S.P. Shankar, S. Waldek, C. Wanner, A. Jovanovic, Phenotypic characteristics of the p.Asn215Ser (p.N215S) GLA mutation in male and female patients with Fabry disease: A multicenter Fabry Registry study, *Mol. Genet. Genom. Med.* (2018). Doi: 10.1002/mgg3.389.
- [54] S. Yamamoto, T. Nagasawa, K. Sugimura, A. Kanno, S. Tatebe, T. Aoki, H. Sato, K. Kozu, R. Konno, K. Nochioka, K. Satoh, H. Shimokawa, Clinical Diversity in Patients with Anderson-fabry Disease with the R301Q Mutation, *Intern. Med.* 58 (2019) 603–607, <https://doi.org/10.2169/internalmedicine.0959-18>.
- [55] W. Dichtl, Echocardiography for clarification of arterial hypertension, accessed June 11, 2024, J. Für Hyperton. - Austrian J. Hypertens. 20 (2016) 94–97, <https://www.kup.at/journals/summary/13712.html>.
- [56] A. Kihara, Sphingosine 1-phosphate is a key metabolite linking sphingolipids to glycerophospholipids, *Biochim. Biophys. Acta BBA - Mol. Cell Biol. Lipids* 1841 (2014) 766–772, <https://doi.org/10.1016/j.bbalip.2013.08.014>.
- [57] S.B. Russo, R. Tidhar, A.H. Futerman, L.A. Cowart, Myristate-derived d16: O sphingolipids constitute a Cardiac Sphingolipid Pool with Distinct Synthetic Routes and Functional Properties, *J. Biol. Chem.* 288 (2013) 13397–13409, <https://doi.org/10.1074/jbc.M112.428185>.
- [58] M. Hilvo, V.C. Vasile, L.J. Donato, R. Hurme, R. Laaksonen, Ceramides and Ceramide Scores: Clinical Applications for Cardiometabolic Risk Stratification, *Front. Endocrinol. Lausanne* 11 (2020) 570628, <https://doi.org/10.3389/fendo.2020.570628>.
- [59] V. Manwaring, M. Boutin, C. Auray-Blais, A Metabolomic Study To Identify New Globotriaosylceramide-Related Biomarkers in the Plasma of Fabry Disease Patients, *Anal. Chem.* 85 (2013) 9039–9048, <https://doi.org/10.1021/ac401542k>.
- [60] M.J. van Breemen, S.M. Rombach, N. Dekker, B.J. Poorthuis, G.E. Linthorst, A. H. Zwinderman, F. Breunig, C. Wanner, J.M. Aerts, C.E. Hollak, Reduction of elevated plasma globotriaosylsphingosine in patients with classic Fabry disease following enzyme replacement therapy, *Biochim. Biophys. Acta BBA - Mol. Basis Dis.* 1812 (2011) 70–76, <https://doi.org/10.1016/j.bbadis.2010.09.007>.
- [61] E. Mårtensson, Neutral glycolipids of human kidney isolation, identification, and fatty acid composition, *Biochim. Biophys. Acta BBA - Lipids Lipid Metab.* 116 (1966) 296–308, [https://doi.org/10.1016/0005-2760\(66\)90012-9](https://doi.org/10.1016/0005-2760(66)90012-9).
- [62] D.E. Vance, W. Krivit, C.C. Sweeley, Concentrations of glycosyl ceramides in plasma and red cells in Fabry's disease, a glycolipid lipidosis, *J. Lipid Res.* 10 (1969) 188–192, [https://doi.org/10.1016/S0022-2275\(20\)42667-7](https://doi.org/10.1016/S0022-2275(20)42667-7).
- [63] J. Spiewak, I. Doykov, A. Papandreou, J. Hällqvist, P. Mills, P.T. Clayton, P. Gissen, K. Mills, W.E. Heywood, New Perspectives in Dried Blood Spot Biomarkers for Lysosomal Storage Diseases, *Int. J. Mol. Sci.* 24 (2023) 10177, <https://doi.org/10.3390/ijms241210177>.
- [64] A.J. Kanack, K. Aoki, M. Tiemeyer, N.M. Dahms, Platelet and myeloid cell phenotypes in a rat model of Fabry disease, *FASEB J* 35 (2021) e21818.
- [65] J.J. Miller, K. Aoki, F. Moehring, C.A. Murphy, C.L. O'Hara, M. Tiemeyer, C. L. Stucky, N.M. Dahms, Neuropathic pain in a Fabry disease rat model, *JCI Insight* 3 (2018), <https://doi.org/10.1172/jci.insight.99171>.
- [66] L.L.W. Cooling, K.E. Walker, T. Gilie, T.A.W. Koerner, Shiga Toxin Binds Human Platelets via Globotriaosylceramide (Pk Antigen) and a Novel Platelet Glycosphingolipid, *Infect. Immun.* 66 (1998) 4355–4366, <https://doi.org/10.1128/IAI.66.9.4355-4366.1998>.
- [67] R. Fisher, The variation in strength of the human blood group P, *Heredity* 7 (1953) 81–90, <https://doi.org/10.1038/hdy.1953.7>.
- [68] L. Stenfelt, Å. Hellberg, J.S. Westman, M.L. Olsson, The P1PK blood group system: revisited and resolved, *Immunohematology* 36 (2020) 99–103, <https://doi.org/10.21307/immunohematology-2020-048>.
- [69] B. Thuresson, J.S. Westman, M.L. Olsson, Identification of a novel A4GALT exon reveals the genetic basis of the P1/P2 histo-blood groups, *Blood* 117 (2011) 678–687, <https://doi.org/10.1182/blood-2010-08-301333>.
- [70] S. Muralidharan, F. Torta, M.K. Lin, A. Olona, M. Bagnati, A. Moreno-Moral, J.-H. Ko, S. Ji, B. Burla, M.R. Wenk, H.G. Rodrigues, E. Petretto, J. Behmoaras, Immunolipidomics Reveals a Globoside Network During the Resolution of Pro-Inflammatory Response in Human Macrophages, accessed August 4, 2022, *Front.*

- Immunol. 13 (2022), <https://www.frontiersin.org/articles/10.3389/fimmu.2022.926220>.
- [71] E. Aflaki, W. Westbroek, E. Sidransky, The complicated relationship between Gaucher disease and Parkinsonism: Insights from a rare disease, *Neuron* 93 (2017) 737–746, <https://doi.org/10.1016/j.neuron.2017.01.018>.
- [72] R.B. Chan, A.J. Perotte, B. Zhou, C. Liang, E.J. Shorr, K.S. Marder, U.J. Kang, C. H. Waters, O.A. Levy, Y. Xu, H.B. Shim, I. Pe'er, G. Di Paolo, R.N. Alcalay, Elevated GM3 plasma concentration in idiopathic Parkinson's disease: A lipidomic analysis, *PLoS One* 12 (2017) e0172348.
- [73] M.F. Gago, O. Azevedo, A. Guimaraes, A. Teresa Vide, N.J. Lamas, T.G. Oliveira, P. Gaspar, E. Bicho, G. Miltenberger-Miltenyi, J. Ferreira, N. Sousa, Parkinson's Disease and Fabry Disease: Clinical, Biochemical and Neuroimaging Analysis of Three Pedigrees, *J Park. Dis* 10 (2020) 141–152, <https://doi.org/10.3233/JPD-191704>.
- [74] A.H. Wise, A. Yang, H. Naik, C. Stauffer, N. Zeid, C. Liang, M. Balwani, R. J. Desnick, R.N. Alcalay, Parkinson's disease prevalence in Fabry disease: A survey study, *Mol Genet Metab Rep* 14 (2018) 27–30, <https://doi.org/10.1016/j.ymgmr.2017.10.013>.
- [75] N. Brakch, O. Dormond, S. Bekri, D. Golshayan, M. Corveon, L. Mazzolai, B. Steinmann, F. Barbey, Evidence for a role of sphingosine-1 phosphate in cardiovascular remodelling in Fabry disease, *Eur. Heart J* 31 (2010) 67–76, <https://doi.org/10.1093/eurheartj/ehp387>.
- [76] R. Brunkhorst, W. Pfeilschifter, S. Patyna, S. Buttner, T. Eckes, S. Trautmann, D. Thomas, J. Pfeilschifter, A. Koch, Preanalytical Biases in the Measurement of Human Blood Sphingolipids, *Int J Mol Sci* 19 (2018), <https://doi.org/10.3390/ijms19051390>.
- [77] P. Hänel, P. Andréani, M.H. Gräler, Erythrocytes store and release sphingosine 1-phosphate in blood, *FASEB J* 21 (2007) 1202–1209, <https://doi.org/10.1096/fj.06-7433com>.
- [78] C. Bode, S.C. Sensken, U. Peest, G. Beutel, F. Thol, B. Levkau, Z. Li, R. Bittman, T. Huang, M. Tolle, M. van der Giet, M.H. Graler, Erythrocytes serve as a reservoir for cellular and extracellular sphingosine 1-phosphate, *J Cell Biochem* 109 (2010) 1232–1243, <https://doi.org/10.1002/jcb.22507>.
- [79] T.M. Vu, A.-N. Ishizu, J.C. Foo, X.R. Toh, F. Zhang, D.M. Whee, F. Torta, A. Cazenave-Gassiot, T. Matsumura, S. Kim, S.-A.-E.-S. Toh, T. Suda, D.L. Silver, M.R. Wenk, L.N. Nguyen, Mfsd2b is essential for the sphingosine-1-phosphate export in erythrocytes and platelets, *Nature* 550 (2017) 524–528, <https://doi.org/10.1038/nature24053>.
- [80] J. Kleinert, F. Dehout, A. Schwarting, A.G. de Lorenzo, R. Ricci, C. Kampmann, M. Beck, U. Ramaswami, A. Linhart, A. Gal, G. Houge, U. Widmer, A. Mehta, G. Sunder-Plassmann, Anemia is a new complication in Fabry disease: data from the Fabry Outcome Survey, *Kidney Int* 67 (2005) 1955–1960, <https://doi.org/10.1111/j.1523-1755.2005.00294.x>.
- [81] S. Selim, M. Sunkara, A.K. Salous, S.W. Leung, E.V. Berdyshev, A. Bailey, C. L. Campbell, R. Charnigo, A.J. Morris, S.S. Smyth, Plasma levels of sphingosine 1-phosphate are strongly correlated with haematocrit, but variably restored by red blood cell transfusions, *Clin. Sci.* 121 (2011) 565–572, <https://doi.org/10.1042/CS20110236>.
- [82] H. Fyrst, J.D. Saba, An update on sphingosine-1-phosphate and other sphingolipid mediators, *Nat. Chem. Biol.* 6 (2010) 489–497, <https://doi.org/10.1038/nchembio.392>.
- [83] E. Kolodny, A. Fellgiebel, M.J. Hilz, K. Sims, P. Caruso, T.G. Phan, J. Politei, R. Manara, A. Burlina, Cerebrovascular Involvement in Fabry Disease, *Stroke* 46 (2015) 302–313, <https://doi.org/10.1161/STROKEAHA.114.006283>.
- [84] J. Liu, K. Sugimoto, Y. Cao, M. Mori, L. Guo, G. Tan, Serum Sphingosine 1-Phosphate (S1P): A Novel Diagnostic Biomarker in Early Acute Ischemic Stroke, *Front Neurol* 11 (2020) 985, <https://doi.org/10.3389/fneur.2020.00985>.
- [85] E. Schwedhelm, L. Schwieren, S. Tiedt, M. von Lucadou, N.O. Gloyer, R. Boger, T. Magnus, G. Daum, G. Thomalla, C. Gerloff, C.U. Choe, Serum Sphingosine-1-Phosphate Levels Are Associated With Severity and Outcome in Patients With Cerebral Ischemia, *Stroke* 52 (2021) 3901–3907, <https://doi.org/10.1161/STROKEAHA.120.033414>.
- [86] J.-J. Aguilera-Correa, P. Madrazo-Clemente, M. del C. Martínez-Cuesta, C. Peláez, A. Ortiz, M.D. Sánchez-Niño, J. Esteban, T. Requena, Lyso-Gb3 modulates the gut microbiota and decreases butyrate production, *Sci. Rep.* 9 (2019) 12010. Doi: 10.1038/s41598-019-48426-4.
- [87] M. Lenders, E. Brand, Fabry disease – a multisystemic disease with gastrointestinal manifestations, *Gut Microbes* 14 (2022) 2027852, <https://doi.org/10.1080/19490976.2022.2027852>.
- [88] A. Wretling, V.R. Curovic, T. Suvitaival, S. Theilade, N. Tofte, S.A. Winther, T. Vilsbøll, H. Vestergaard, P. Rossing, C. Legido-Quigley, Ceramides as Risk Markers for Future Cardiovascular Events and All-Cause Mortality in Long-standing Type 1 Diabetes, *Diabetes* 72 (2023) 1493–1501, <https://doi.org/10.2337/db23-0052>.
- [89] A.S. Havulinna, M. Sysi-Aho, M. Hilvo, D. Kauhanen, R. Hurme, K. Ekroos, V. Salomaa, R. Laaksonen, Circulating Ceramides Predict Cardiovascular Outcomes in the Population-Based FINRISK 2002 Cohort, *Arterioscler. Thromb. Vasc. Biol.* 36 (2016) 2424–2430. Doi: 10.1161/ATVBAHA.116.307497.
- [90] L.R. Peterson, V. Xanthakis, M.S. Duncan, S. Gross, N. Friedrich, H. Völzke, S.B. Felix, H. Jiang, R. Sidhu, M. Nauck, X. Jiang, D.S. Ory, M. Dörr, R.S. Vasan, J.E. Schaffer, Ceramide Remodeling and Risk of Cardiovascular Events and Mortality, *J. Am. Heart Assoc.* 7 (n.d.) e007931. Doi: 10.1161/JAHA.117.007931.
- [91] A.S. Papazoglou, N. Stalikas, D.V. Moysidis, N. Otoutzidis, A. Kartas, E. Karagiannidis, G. Giannakoulas, G. Sianos, CERT2 ceramide- and phospholipid-based risk score and major adverse cardiovascular events: A systematic review and meta-analysis, *J. Clin. Lipidol.* 16 (2022) 272–276, <https://doi.org/10.1016/j.jacl.2022.02.001>.
- [92] J.B. Augusto, S. Nordin, R. Vijapurapu, S. Baig, H. Bulluck, S. Castelletti, M. Alfarihi, K. Knott, G. Captur, T. Kotecha, U. Ramaswami, M. Tchan, T. Geberhiwot, M. Fontana, R.P. Steeds, D. Hughes, R. Kozor, J.C. Moon, Myocardial Edema, Myocyte Injury, and Disease Severity in Fabry Disease, *Circ. Cardiovasc. Imaging* 13 (2020) e010171.
- [93] M. Siegenthaler, U. Huynh-Do, P. Krayenbuehl, E. Pollock, U. Widmer, H. Debaix, E. Olinger, M. Frank, M. Namdar, F. Ruschitzka, A. Nowak, Impact of cardio-renal syndrome on adverse outcomes in patients with Fabry disease in a long-term follow-up, *Int J Cardiol* 249 (2017) 261–267, <https://doi.org/10.1016/j.ijcard.2017.09.027>.
- [94] X. Fan, Y. Wang, X. Cai, Y. Shen, T. Xu, Y. Xu, J. Cheng, X. Wang, L. Zhang, J. Dai, S. Lin, J. Liu, CPT2 K79 acetylation regulates platelet life span, *Blood Adv.* 6 (2022) 4924–4935, <https://doi.org/10.1182/bloodadvances.2021006687>.
- [95] E. Aflaki, P. Doddapattar, B. Radovic, S. Povoden, D. Kolb, N. Vujic, M. Wegscheider, H. Koefeler, T. Hornemann, W.F. Graier, R. Malli, F. Madeo, D. Kratky, C16 ceramide is crucial for triacylglycerol-induced apoptosis in macrophages, *Cell Death Dis* 3 (2012) e280.
- [96] B. Fekry, K.A. Jeffries, A. Esmaeiliakooshkghazi, Z.M. Szulc, K.J. Knagge, D. R. Kirchner, D.A. Horita, S.A. Krupenko, N.I. Krupenko, C16-ceramide is a natural regulatory ligand of p53 in cellular stress response, *Nat. Commun.* 9 (2018) 4149, <https://doi.org/10.1038/s41467-018-06650-y>.
- [97] A.K. Rudd, N.K. Devaraj, Traceless synthesis of ceramides in living cells reveals saturation-dependent apoptotic effects, *Proc. Natl. Acad. Sci.* 115 (2018) 7485–7490, <https://doi.org/10.1073/pnas.1804266115>.
- [98] M. Chatterjee, D. Rath, J. Schlotterbeck, J. Rheinlaender, B. Walker-Allgaier, N. Alnaggar, M. Zdanyte, I. Müller, O. Borst, T. Geisler, T.E. Schäffer, M. Lämmerhofer, M. Gawaz, Regulation of oxidized platelet lipidome: implications for coronary artery disease, *Eur. Heart J* 38 (2017) 1993–2005, <https://doi.org/10.1093/eurheartj/ehx146>.
- [99] G. Pei, J. Zyla, L. He, P. Moura-Alves, H. Steinle, P. Saikali, L. Lozza, N. Nieuwenhuizen, J. Weiner, H.-J. Mollenkopf, K. Ellwanger, C. Arnold, M. Duan, Y. Dagil, M. Pashenkov, I.G. Boneca, T.A. Kufer, A. Dorhoi, S. H. Kaufmann, Cellular stress promotes NOD1/2-dependent inflammation via the endogenous metabolite sphingosine-1-phosphate, *EMBO J.* 40 (2021) e106272.
- [100] F. Ducatez, W. Mauhin, A. Boullier, C. Pilon, T. Pereira, R. Aubert, O. Benveniste, S. Marret, O. Lidove, S. Bekri, A. Tebani, Parsing Fabry Disease Metabolic Plasticity Using Metabolomics, *J. Pers. Med.* 11 (2021) 898, <https://doi.org/10.3390/jpm11090898>.
- [101] H.B. Beyene, G. Olshansky, A.A.T. Smith, C. Giles, K. Huynh, M. Cinel, N. A. Mellett, G. Cadby, J. Hung, J. Hui, J. Beilby, G.F. Watts, J.S. Shaw, E.K. Moses, D.J. Magliano, P.J. Meikle, High-coverage plasma lipidomics reveals novel sex-specific lipidomic fingerprints of age and BMI: Evidence from two large population cohort studies, *PLoS Biol.* 18 (2020) e3000870.
- [102] S.M. Hammad, J.S. Pierce, F. Soodavar, K.J. Smith, M.M.A. Gadban, B. Rembiesa, R.L. Klein, Y.A. Hannun, J. Bielawski, A. Bielawska, Blood sphingolipidomics in healthy humans: impact of sample collection methodology, *J. Lipid Res.* 51 (2010) 3074–3087, <https://doi.org/10.1194/jlr.D008532>.